Journal of Sound and Vibration (2002) 253(3), 545–569
doi:10.1006/jsvi.2001.3747, available online at http://www.idealibrary.com on IDEAL®

ACTIVE CONTROL OF FLEXIBLE STRUCTURES USING PRINCIPAL COMPONENT ANALYSIS IN THE TIME DOMAIN

A. S. Al-Dmour and K. S. Mohammad

College of Engineering, Mu'tah University, Mu'tah P.O. Box 7, Karak, Jordan.
E-mail: aldmour@mutah.edu.jo

(*Received* 4 *July* 2000, *and in final form* 27 *February* 2001)

Principal component analysis is used to simplify the extraction of the natural frequencies and their corresponding orthonormal mode shapes directly from experimental data of unknown flexible structures. A control law is designed using a state-space modal model and is tested on different structures. The results are extremely encouraging and demonstrate successful implementation of the active control strategies. The controller actuator as well as the detection sensor locations are examined throughout the structure length.

1. INTRODUCTION

Vibration problems are connected basically with oscillatory motion of bodies. These bodies are capable of some level of vibration when they are induced into motion by forces. Most of these vibrations are undesirable due to their destructive and disturbing characteristics. The dynamics of such systems are governed by partial differential equations and understanding these is important for analyzing and modelling the system in order to choose the suitable control laws for damping the unwanted vibration associated with the structure's resonant modes. The best scheme is clearly the one that efficiently cancels these unwanted vibrations.

Passive damping schemes can be considered as a "redesign" process which involves altering the flexible structures' physical parameters, namely, stiffness and damping, to produce the desired response. Sometimes, however, the desired response cannot be obtained using such schemes, especially at low frequencies or when wideband applications are considered [1]. The main reasons for this are economic ones, and the problems of mechanical resonance. Under these circumstances, the alternative is to use active methods.

Active methods usually use external adjustable active devices (actuators) to provide a way of dynamically shaping or controlling the response. These components offer a number of advantages over the passive damping methods, namely the ease with which the frequency bandwidth can be reshaped and their low weight and cost [2]. There are many types of active methods that can be considered for obtaining a suitable control law; these include PID, dead beat, neural networks, fuzzy logic control, optimal control, and state-space control techniques. Information on the wider aspects of vibration control can be found in the works of Al-Dmour [1], Pao and Franklin [3], Dosch *et al.* [4], Sievers and Von Flotow [5], Snyder and Tanaka [6] and Zhang *et al.* [7]. Usually, numerical methods are used for performing the simulation studies of the oscillatory structures; these mainly include modal superposition method, finite-difference and finite-element techniques [1, 8–10]. In principle, flexible structures systems require an infinite number of modes to describe completely their

0022-460X/02/$35.00

behavior. The fundamental problem is to design a suitable control law that can deal with a large dimensionality especially when dealing with digital computer-controlled applications. Thus, it is common to restrict the analysis to few modes, so that the required system performance is achieved in respect of sensitivity, excitation and vibration tolerances. Some of these aspects are discussed by Kourmoulis [9], Porter and Crossley [11], Balas [12], Toki and Hossain [13], Virk and Al-Dmour [14] and Al-Dmour [15, 16]. Consequently, state-space formulations have been used to model vibration problems in a modal basis with prior knowledge of the structure parameters [17–20].

The knowledge of the natural frequencies and their corresponding mode shapes are the core for the successful state-space representation of active controllers. There are many methods which have been developed to extract such parameters from experimental measured data [21, 22]. In particular, the principal component analysis (PCA) method has a unique property for transforming directly a given correlated measured data to a new non-correlated set of data which simplify the parameter estimation of flexible structures [23, 24].

All the methods based on state-space controller used before, require the knowledge of the structure characteristics to be executed. However, as the PCA provides a procedure that can be implemented successfully to extract the system natural frequencies and their corresponding mode shapes from measured data, a new approach based on such a method can be developed to perform these control techniques without prior knowledge of the model.

In this paper, an optimal control technique is considered to deal with the unwanted vibration in different structures, namely, multi-degree-of-freedom (d.o.f.) systems, and a simply-supported beam. These structures are considered as illustrative applications for the present study since they provide the essential principles behind many flexible structures such as aircraft fuselage oscillations, helicopter rotor blades, bridge vibrations, and robotic manipulator systems. In addition, a state-space model is utilized to generate a modal-based solution where the state vector of the model is used to generate the controlling signal. Here, the calculation of modal parameters, namely, mode shapes, and natural frequencies of the considered flexible structures are obtained using the statistical procedure PCA. PCA is used in this paper since it is effectively found to produce single d.o.f. data with well-separated resonances, and minimize the effect of residual modes (i.e., modes outside the frequency range of interest) in the response even in the presence of noise [24].

Before discussing the vibration control of the above-mentioned structures, it is necessary to provide a brief introduction of the mathematical development of the principal component analysis from a statistical point of view, system model and optimal control techniques. This summary is useful for providing the notation used in the paper.

2. PRINCIPAL COMPONENT ANALYSIS

The geometric interpretation for the PCA method will give a clear picture of the basis for developing a mathematical model. Let us assume that two related variables x_1, x_2 are plotted as points in the X_1–X_2 plane as illustrated in Figure 1.

Two variables y_1, y_2 can be determined when the co-ordinates X_1, X_2 are rotated by an angle α which is denoted by Y_1, Y_2; the y_1, y_2 variables can be related to the x_1, x_2 variables by utilizing the expressions

$$y_1 = x_1 \cos\alpha + x_2 \sin\alpha, \qquad y_2 = -x_1 \sin\alpha + x_2 \cos\alpha. \qquad (2.1, 2.2)$$

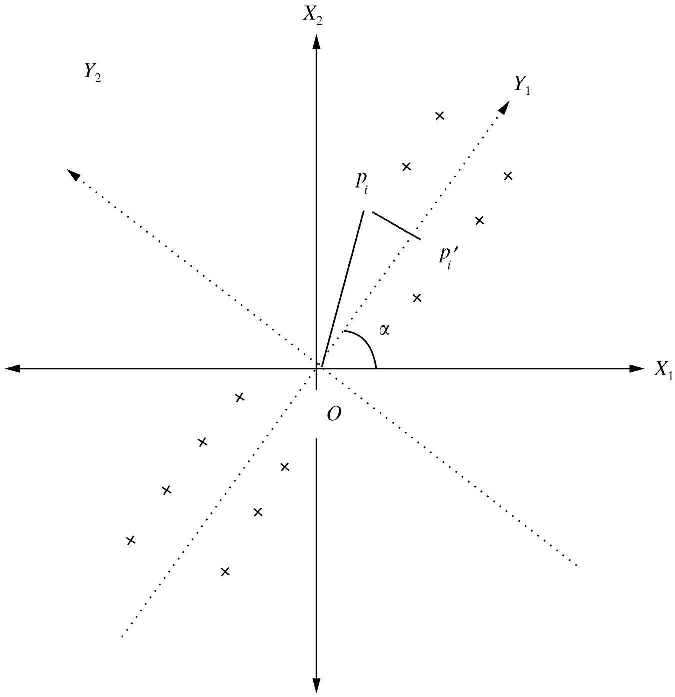

Figure 1. Geometrical representation of the principle component procedure.

It is clear from Figure 1 that the points have a wide distribution pattern along Y_1 while little distribution occurs along Y_2. As a result, choosing a specific value of the angle can result in maximizing the distribution along Y_1 as well as minimizing it along Y_2. This leads to the possibility of representing the data by only one co-ordinate, i.e., one variable. To define the line OY_1, one starts by representing the ith-sampled data with the formulae [25, 26]

$$(op_i)^2 = (op_i')^2 + (pp_i')^2, \quad i = 1, \ldots, N_p, \tag{2.3}$$

where $p_i p_i'$ is the perpendicular distance from the point p_i to the line OY_1 and N_p is the number of sampled points. The summation over all the data points after dividing the results by $N_p - 1$ yields

$$\frac{1}{(N_p - 1)} \sum_{i=1}^{N_p} (op_i)^2 = \frac{1}{(N_p - 1)} \sum_{i=1}^{N_p} (op_i')^2 + \frac{1}{(N_p - 1)} \sum_{i=1}^{N_p} (p_i p_i')^2 \tag{2.4}$$

or

$$(\text{var})_{total} = (\text{var})_1 + (\text{var})_2. \tag{2.5}$$

The terms in equation (2.4) represent the variances of each variable given in equation (2.5).

One can deduce from the graph that the term on the left-hand side of equation (2.1) is constant irrespective of the location of OY_1. Consequently, the best position of OY_1 may be accomplished by minimizing $(\text{var})_2$, and this process is actually equivalent to maximizing $(\text{var})_1$.

This idea is explored and utilized as a starting point for the mathematical modelling of PCA [26]. By assuming that a vector of dimension $(p \times 1)$ with the elements $\{x_1, x_2, \ldots, x_p\}^T$ is collected for N_p samples the variance of the ith variable was expressed by Mohammad [24] as

$$s_{it} = \frac{1}{(N_p - 1)} \sum_{j-1}^{N_p} (x_i - \bar{x}_i)^2, \tag{2.6}$$

where, $\bar{x}_i$ is the mean of the ith variable, and the covariance between the ith and the jth variables is

$$s_{ij} = \frac{1}{(N_p - 1)} \sum_{k-1}^{N_p} (x_{ki} - \bar{x}_i)(x_{jk} - \bar{x}_i). \tag{2.7}$$

Thus, one can build a covariance matrix [**S**] of dimension $(p \times p)$ where its elements are the calculated variances and covariances. Therefore, the matrix [**S**] can be expressed by

$$[\mathbf{S}] = \frac{1}{(N_p - 1)} \left[\sum_{i=1}^{N_p} (\{\mathbf{X}\}_i - \{\bar{\mathbf{X}}\})(\{\mathbf{X}\}_i - \{\bar{\mathbf{X}}\})^T \right]. \tag{2.8}$$

The first principal component Y_1 can be constructed by a linear combination of the given p variables $\{x_1, x_2, \ldots, x_p\}^T$,

$$Y_1 = a_{11}x_1 + a_{21}x_2 + \cdots + a_{p1}x_p \quad \text{or } Y_1 = \{\mathbf{a}\}_1^T \{\mathbf{X}\} \tag{2.9, 2.10}$$

under the constraint

$$\{\mathbf{a}\}_1^T \{\mathbf{a}\}_1 = 1. \tag{2.11}$$

The mean and the variance of Y_1 can be calculated using the respective equations

$$\bar{y}_1 = \{\mathbf{a}\}_1^T \{\bar{\mathbf{X}}\}, \qquad v_{y1} = \{\mathbf{a}\}_1^T [\mathbf{S}] \{\mathbf{a}\}_1. \tag{2.12, 2.13}$$

The best position of Y_1 can be found by maximizing the variance v_{y1}. Lagrange multiplication procedure is utilized to achieve this goal [27]. A new function V_1 is constructed having the form

$$V_1 = \{\mathbf{a}\}_1^T [\mathbf{S}] \{\mathbf{a}\}_1 + \lambda_1 (1 - \{\mathbf{a}\}_1^T \{\mathbf{a}\}_1), \tag{2.14}$$

where λ_1 is the Lagrange multiplier coefficient. The elements of the vector $\{\mathbf{a}\}_1$, and λ_1 that maximize v_{y1} can be obtained by differentiating equation (2.14) with respect to each element of $\{\mathbf{a}\}_1$ and equating the results to zero. The differentiation of V_1 with respect to the ith element of $\{\mathbf{a}\}_1$ is

$$\partial V_1 / \partial a_{k1} = [2a_{k1}[\mathbf{S}] - 2\lambda_1 a_{k1}] = 0{\cdot}0. \tag{2.15}$$

The p differentiation equations can be gathered in a matrix that has the form

$$([\mathbf{S}] - \lambda_1 [\mathbf{I}]) \{\mathbf{a}\}_1 = \{\mathbf{0}\}, \tag{2.16}$$

where [**I**] is the unity matrix. Thus, λ_1 is one of the roots of the characteristic equation $([\mathbf{S}] - \lambda[\mathbf{I}])$ and $\{\mathbf{a}\}_1$ its corresponding eigenvector. To obtain λ_1, one should multiply equation (2.16) by $\{\mathbf{a}\}_1^{\mathrm{T}}$ which results in

$$\{\mathbf{a}\}_1^{\mathrm{T}}[\mathbf{S}]\{\mathbf{a}\}_1 - \lambda\{\mathbf{a}\}_1^{\mathrm{T}}\{\mathbf{a}\}_1 = 0, \tag{2.17}$$

since

$$\{\mathbf{a}\}_1^{\mathrm{T}}\{\mathbf{a}\}_1 = 1, \qquad \text{therefore } \lambda_1 = \{\mathbf{a}\}_1^{\mathrm{T}}[\mathbf{S}]\{\mathbf{a}\}_1, \tag{2.18, 2.19}$$

but as

$$v_{y1} = \{\mathbf{a}\}_1^{\mathrm{T}}[\mathbf{S}]\,\{\mathbf{a}\}_1, \qquad \lambda_1 = v_{y1}. \tag{2.20, 2.21}$$

As the aim of this procedure is to maximize v_{y1}, λ_1 is found to be the greatest root of the matrix [**S**]. The second principal component Y_2 may be obtained using similar steps that are adapted for determining Y_2 but with extra constraint, to ensure that Y_2 is orthogonal to Y_1, and a maximum of the remaining $p-1$ variables. Thus, Y_2 may be expressed by

$$Y_2 = a_{21}x_1 + a_{22}x_2 + \cdots + a_{2p}x_p \qquad \text{or } Y_2 = \{\mathbf{a}\}_2^{\mathrm{T}}\{\mathbf{X}\} \tag{2.22, 2.23}$$

with the constraints

$$\{\mathbf{a}\}_2^{\mathrm{T}}\{\mathbf{a}\}_2 = 1 \quad \text{and} \quad \{\mathbf{a}\}_1^{\mathrm{T}}\{\mathbf{a}\}_2 = 0. \tag{2.24, 2.25}$$

A function is constructed with two Lagrange multipliers as

$$V_2 = \{\mathbf{a}\}_2^{\mathrm{T}}[\mathbf{S}]\{\mathbf{a}\}_2 + \lambda_2(1 - \{\mathbf{a}\}_2^{\mathrm{T}}\{\mathbf{a}\}_2) + \mu\{\mathbf{a}\}_1^{\mathrm{T}}\{\mathbf{a}\}_2. \tag{2.26}$$

Differentiating equation (2.26) with respect to each element of the vector $\{\mathbf{a}\}_2$ the result is then equated to zero and gathered in the matrix

$$([\mathbf{S}] - \lambda_2[\mathbf{I}])\{\mathbf{a}\}_2 - \mu\{\mathbf{a}\}_1 = \{\mathbf{0}\}. \tag{2.27}$$

To find μ, multiply equation (2.27) by $\{\mathbf{a}\}_1^{\mathrm{T}}$ with the result that

$$\{\mathbf{a}\}_1^{\mathrm{T}}[\mathbf{S}]\{\mathbf{a}\}_2 - \lambda_2\{\mathbf{a}\}_1^{\mathrm{T}}\{\mathbf{a}\}_2 - \{\mathbf{a}\}_1^{\mathrm{T}}\{\mathbf{a}\}_1 = 0 \tag{2.28}$$

and since

$$\{\mathbf{a}\}_1^{\mathrm{T}}[\mathbf{S}]\{\mathbf{a}\}_2 = 0, \quad \{\mathbf{a}\}_1^{\mathrm{T}}\{\mathbf{a}\}_2 = 0, \tag{2.29, 2.30}$$

Therefore,

$$\mu = 0. \tag{2.31}$$

Thus, equation (2.26) becomes

$$([\mathbf{S}] - \lambda_2[\mathbf{I}])\{\mathbf{a}\}_2 = \{\mathbf{0}\}. \tag{2.32}$$

This is similar to equation (2.16). It follows that λ_2 is the second largest root of [**S**] which is equal to v_{y2}, and $\{\mathbf{a}\}_2$ is its corresponding eigenvector. Consequently, in general the ith principal component Y_i can be constructed as a linear combination of the p variables $\{x_1, x_2, \ldots, x_p\}^{\mathrm{T}}$, i.e.,

$$Y_i = \{\mathbf{a}\}_1^{\mathrm{T}}\{\mathbf{X}\}, \quad i = 1, \ldots, p, \tag{2.33}$$

where $\{\mathbf{a}\}_i$ is the eigenvector of the ith eigenvalue λ_i of the matrix [**S**], and λ_i is equal to the variance v_{y1}; this deduction can be written in matrix form as

$$[\mathbf{U}]^{\mathrm{T}}[\mathbf{S}][\mathbf{U}] = [\mathbf{\Sigma}], \tag{2.34}$$

where [**U**] is a matrix of p orthonormal eigenvectors of dimension $(p \times p)$ and $[\mathbf{\Sigma}]$ is a diagonal matrix with eigenvalues of [**S**], of dimension $(p \times p)$.

Since the inverse of the orthogonal matrix is equal to its transpose, equation (2.34) can be rewritten as

$$[\mathbf{S}] = [\mathbf{U}][\mathbf{\Sigma}][\mathbf{U}]^{\mathrm{T}}. \tag{2.35}$$

Furthermore, the singular value decomposition (SVD) technique is a numerical procedure which factorizes a given matrix [**A**] of dimension $(p \times p)$ into the following form [28]:

$$[\mathbf{A}] = [\mathbf{U}][\mathbf{\Sigma}][\mathbf{U}]^{\mathrm{T}}. \tag{2.36}$$

Thus, the SVD technique can be used as a tool on the matrix [**S**] to specify the PCA variables $\{y_1, y_2, \dots, y_p\}$. The factorization of the covariance matrix [**S**] indicates that the correlated p variables can be transformed to new, non-correlated, p-principal variables. As examination of the values of the diagonal matrix $\mathbf{\Sigma}$ may reveals that the magnitude of the variances v_{y1}, where $r < i < p$, is so small that it can be ignored. Thus, the diagonal elements of the $\mathbf{\Sigma}$ matrix have the values

$$\mathbf{\Sigma} = \begin{cases} \lambda_i = v_{y1}, & 1 \leqslant i \leqslant r, \\ \lambda_i = 0{\cdot}0, & r \leqslant i \leqslant p. \end{cases} \tag{2.37}$$

As a result, it is possible to represent the matrix [**S**], without losing important information in the data, approximately by

$$[\mathbf{S}] \cong [\mathbf{U}]'[\mathbf{\Sigma}]'[\mathbf{U}]^{\mathrm{T}}, \tag{2.38}$$

where $[\mathbf{U}]'$ is the orthonormal matrix of dimension $(p \times r)$ and $[\mathbf{\Sigma}]$ is the diagonal matrix of dimension $(r \times r)$.

Consequently, one can transform the correlated p variables to r non-correlated principal variables.

2.1. PRINCIPAL TIME RESPONSE FUNCTIONS

Consider a linear continuous flexible structure modelled by an N_0 d.o.f. lumped system. The displacement output responses of such a structure when excited by a step disturbance force at N_i locations, where $N_i < N_0$, can be obtained by

$$\{\mathbf{X}(t)\} = \sum_{j=1}^{N_0} \{\mathbf{\Psi}\}_j \, CA_j \sin\left(\omega_{nj} + \frac{\pi}{2}\right) + \{x_p(t)\}, \tag{2.39}$$

where $\{\mathbf{X}(t)\}$ is the displacement vector of dimension $(N_0 \times 1)$; $\{\mathbf{\Psi}\}_j$ is the jth column of the normalized mode shape matrix $[\mathbf{\Psi}]$ of dimension $(N_0 \times 1)$, ω_{nj} is the jth natural frequency of the system, CA_j is the jth element of the amplitude vector $\{\mathbf{CA}\}$, with $\{\mathbf{CA}\} = -1 \times [\mathbf{\Psi}]^{-1}[\mathbf{k}]^{-1}\{\mathbf{f}(t)\}$, $[\mathbf{k}]$ is the stiffness matrix of dimension $(N_0 \times N_0)$, $\{\mathbf{f}(t)\}$ is the applied force vector of dimension $(N_0 \times 1)$, $\{\mathbf{x}_p(t)\}$ is the steady state displacement vector of dimension $(N_0 \times 1)$ and is equal to $[\mathbf{k}]^{-1}\{\mathbf{f}(t)\}$.

These responses are recorded for N_p sampled points and then the matrix $[\mathbf{S}]_{gg}$ can be calculated from the collected data as follows:

$$[\mathbf{S}]_{gg} = [\mathbf{X}][\mathbf{X}]^{\mathrm{T}} \text{ of dimension } (N_0 \times N_0), \tag{2.40}$$

where $[\mathbf{X}]$ is the time response data matrix for the N_0 locations, of dimension $(N_0 \times N_p)$. The matrix $[\mathbf{S}]_{gg}$ is an equivalent representation of the covariance matrix $[\mathbf{S}]$. Consequently, one can factorize $[\mathbf{S}]_{gg}$ using SVD procedure as

$$[\mathbf{S}]_{gg} = [\mathbf{U}][\boldsymbol{\Sigma}][\mathbf{U}]^{\mathrm{T}}. \tag{2.41}$$

As a result, the factorization of $[\mathbf{S}]_{gg}$ will reveal N_0 singular values that have significant magnitudes, which can be obtained from the $[\boldsymbol{\Sigma}]$ matrix. Thus, the generalized N_0 co-ordinates can be transformed to N_0 non-correlated principal co-ordinates, i.e.,

$$\{\mathbf{X}\}_p = [\mathbf{U}]^{\mathrm{T}}\{\mathbf{X}\}, \tag{2.42}$$

where $\{\mathbf{X}\}$ is the correlated responses vector, of dimension $(N_0 \times 1)$, $\{\mathbf{X}\}_p$ is the non-correlated responses vector of dimension $(N_0 \times 1)$, and the data set for the non-correlated responses can be expressed in matrix form as

$$[\mathbf{X}]_p = [\mathbf{U}]^{\mathrm{T}}[\mathbf{X}] \quad \text{of dimension } (N_0 \times N_p). \tag{2.43}$$

However, in practice the number of d.o.f. N_r measured is usually less than the number of response locations N_0. Now, the matrix $[\boldsymbol{\Sigma}]$, which resulted from factorizing the $[\mathbf{S}]_{gg}$ matrix, will reveal only the first N_r singular values with significant magnitudes. Thus, it is possible, without losing valuable information, to represent approximately $[\mathbf{S}]_{gg}$ by

$$[\mathbf{S}]_{gg} \cong [\mathbf{U}]'[\boldsymbol{\Sigma}]'[\mathbf{U}]'^{\mathrm{T}}. \tag{2.44}$$

Consequently, the $[\mathbf{U}]'$ matrix can be used to transform the generalized N_0 co-ordinates to N_r non-correlated principal co-ordinates applying the following formulae:

$$\{\mathbf{X}\}_p = [\mathbf{U}]^{\mathrm{T}}\{\mathbf{X}\} \quad \text{of dimension } (N_r \times 1), \tag{2.45}$$

$$\{\mathbf{X}\}_p = [\mathbf{U}]^{\mathrm{T}}\{\mathbf{X}\} \quad \text{of dimension } (N_r \times N_p). \tag{2.46}$$

A similar representation of $[\mathbf{S}]_{gg}$ can be obtained when a measured data of real structures are recorded. The $[\mathbf{X}]_p$ eigenvector matrix and the estimated natural frequencies that are found from the non-correlated single d.o.f. data are utilized in generating the required control signals for suppressing the vibration of the considered structures.

3. MODEL DESCRIPTION OF FLEXIBLE SYSTEMS

Undamped flexible system can be modelled in matrix form by using the differential equation [20]

$$[\mathbf{M}]\{\ddot{\mathbf{q}}\} + [\mathbf{K}]\{\mathbf{q}\} = \{\mathbf{f}\}, \tag{3.1}$$

where $[\mathbf{M}]$ and $[\mathbf{K}]$ are generalized mass and stiffness matrices of the structure, $\{\ddot{\mathbf{q}}\}$ and $\{\mathbf{q}\}$ are vectors of acceleration and displacement of the nodal points of the structure, and $\{\mathbf{f}\}$ is a vector of external forces acting on the structure.

Equation (3.1) can be put in modal space in order to simplify the analysis for determining the solution by using the well-known modal transformation [17, 18] as

$$\{\mathbf{q}\} = [\mathbf{\Phi}]\{\mathbf{u}\}, \tag{3.2}$$

where $\{\mathbf{u}\}$ is a vector of modal co-ordinate of the system, and $[\mathbf{\Phi}]$ is the mass normalized mode shape matrix, normalized such that

$$[\mathbf{\Phi}]^{\mathrm{T}}[\mathbf{M}][\mathbf{\Phi}] = \mathrm{I}. \tag{3.3}$$

With such a transformation, equation (3.1) can then be transformed into the uncoupled form

$$\{\ddot{\mathbf{u}}\} + [\mathbf{\Omega}]\{\mathbf{u}\} = [\mathbf{\Phi}]^{\mathrm{T}}\{\mathbf{f}\}, \tag{3.4}$$

where $[\mathbf{\Omega}]$ is the modal frequency matrix, given by

$$[\mathbf{\Omega}] = [\mathbf{\Phi}]^{\mathrm{T}}[\mathbf{K}][\mathbf{\Phi}] = \text{diag.}\ \{\omega_i^2\}, \quad i = 1, \ldots, N, \tag{3.5}$$

where N is the number of modes of the flexible system under consideration.

Here, the mode shapes and the modal frequencies are both found from the PCA procedure discussed in section 2. It should be noted here that these equations are developed by assuming zero structural damping. The modal equations can then be written in the standard state-space forms as

$$\{\dot{\mathbf{z}}\} = [\mathbf{A}]\{\mathbf{z}\} + \{\mathbf{B}\}f_c + \{\mathbf{D}\}f_d, \qquad y = Cz, \tag{3.6, 3.7}$$

where

$$\{\mathbf{z}\} = \begin{Bmatrix} u \\ \dot{u} \end{Bmatrix}, \quad A = \begin{bmatrix} 0 & 1 \\ \omega^2 i & 0 \end{bmatrix} \quad (i = 1, 2, \ldots, N)$$

is the ith mode model matrix; f_c and f_d are the control and disturbance forces acting on the structure respectively;

$$\{\mathbf{B}\} = \begin{Bmatrix} 0 \\ \Phi_i(\alpha_c) \end{Bmatrix} \quad \text{and} \quad \{\mathbf{D}\} = \begin{Bmatrix} \mathbf{0} \\ \Phi_i(\alpha_d) \end{Bmatrix} \quad (i = 1, 2, \ldots, N)$$

are the control and disturbance input vectors placed at location α_c and α_d on the structure respectively and

$$C = \begin{bmatrix} \Phi_i(\alpha_{ds}) & 0 \\ 0 & \Phi_i(\alpha_{vs}) \end{bmatrix} \quad (i = 1, 2, \ldots, N)$$

is the output matrix for displacement (or deflection) and velocity sensors placed at location α_{ds} and α_{vs} on the structure respectively.

Therefore, equation (3.6) can be partitioned into $N 2 \times 2$ state-space representation for one-control point and one-disturbance point forces so that they can be solved on a computer system as

$$\begin{bmatrix} \dot{z}_l \\ \dot{z}_{l-N} \end{bmatrix} = \begin{bmatrix} 0 & 1 \\ -\omega_l^2 & 0 \end{bmatrix} \begin{bmatrix} z_l \\ z_{l-N} \end{bmatrix} + \begin{bmatrix} 0 \\ \Phi_i(\alpha_c) \end{bmatrix} f_{ci} + \begin{bmatrix} 0 \\ \Phi_i(\alpha_d) \end{bmatrix} f_{dl}, \quad i = 1, 2, \ldots, N. \tag{3.8}$$

Equation (3.8) represents N second order state-space blocks with each representing a decoupled mode. It is these equations that will be utilized to model the structure system behavior and to derive state-space control laws for suppressing the vibration of the considered structures.

4. LINEAR STATE FEEDBACK CONTROLLERS

In many practical cases, only a limited number of effective (or dominant) modes are excited. The objective of active damping is to suppress the vibration of such dominant modes. The controller design methodology is proposed to determine the feedback gains and then compute that suitable control signal that is applied to a control actuator placed in a suitable location at the flexible structure. The generation of the control signal is based upon the response calculated by velocity responses. Here, adding damping to the undamped structure system presented in equation (3.1) controls the vibration problem. It is known that the linear quadratic theory is one of the most efficient approaches that can be used with the state-space model for generating an optimal control signal [29]. The approach procedure is to minimize a linear quadratic cost index donated J which is given in reference [30] as

$$J = \int_0^\infty (\{\mathbf{z}\}^{\mathrm{T}}[\mathbf{C}]^{\mathrm{T}}[\mathbf{Q}][\mathbf{C}]\{\mathbf{z}\} + \{\mathbf{f}_c\}^{\mathrm{T}}[\mathbf{R}]\{\mathbf{f}_c\})\,\mathrm{d}t, \tag{4.1}$$

where $[\mathbf{Q}]$ and $[\mathbf{R}]$ are positive-definite diagonal weighting matrices. It is well-known that the solution to the above minimization problem is given by the linear feedback control law

$$f_c(t) = -[\mathbf{R}]^{-1}\{\mathbf{B}\}^{\mathrm{T}}[\mathbf{P}]\{\mathbf{z}\}, \tag{4.2}$$

where matrix $[\mathbf{P}]$ depends on the solution of the Riccati equation which is expressed in reference [20] by

$$[\mathbf{P}][\mathbf{A}] + [\mathbf{A}]^{\mathrm{T}}[\mathbf{P}] - [\mathbf{P}]\{\mathbf{B}\}[\mathbf{R}]^{-1}[\mathbf{B}]^{\mathrm{T}}[\mathbf{P}] + [\tilde{\mathbf{Q}}] = [\dot{\mathbf{P}}], \tag{4.3}$$

where $[\tilde{\mathbf{Q}}] = [\mathbf{C}]^{\mathrm{T}}[\mathbf{Q}][\mathbf{C}]$ and $[\mathbf{R}]$ is chosen such that $[\tilde{\mathbf{Q}}]/[\mathbf{R}] \Rightarrow \infty$ [9]. Since it is desirable to have constant feedback gains in the vibration control system of time-invariant structures' parameters, only the steady state value of the Riccati equation will be used in this work. Therefore, this leads to the value of $\dot{\mathbf{P}}$ being zero.

5. SIMULATION RESULTS

Active control methods for vibration suppression are considered to offer a good generic methodology. The overall procedure to be carried out is to measure the output displacement (or velocity) of the structure using suitable sensors. A state-space model is utilized to generate the state vector that is needed in calculating the feedback control signal. Then, the resulting signal is applied to the control actuator. This procedure needs to be repeated continuously at an appropriate sampling rate.

The presented approaches discussed in sections 3 and 4 are used to suppress the vibration of the dominant modes of different unknown structures, namely, three and five (d.o.f.) systems, and simply supported beam. To demonstrate the active vibration suppression of such structure systems, the natural frequencies, and mode shapes need to be carefully examined so that good vibration suppression can be achieved.

5.1. A THREE-d.o.f. SYSTEM

A three d.o.f. system having the mass and stiffness matrices

$$[\mathbf{m}] = \begin{bmatrix} 1 & 0 & 0 \\ 0 & 1 & 0 \\ 0 & 0 & 1 \end{bmatrix} (\text{Kg}), \quad [\mathbf{k}] = \begin{bmatrix} 2 & -1 & 0 \\ -1 & 2 & -1 \\ 0 & -1 & 2 \end{bmatrix} (\text{N m}^{-1} \times 10^4),$$

is used to demonstrate the validity of the presented approach in section 2. The natural frequencies and their corresponding normalized mode shapes are calculated using the iterative method [31]. These are

$$f_{n1} = 12{\cdot}1812\ \text{Hz}, \quad f_{n2} = 22{\cdot}4743\ \text{Hz}, \quad f_{n3} = 29{\cdot}408\ \text{Hz} \quad \text{and}$$

$$[\boldsymbol{\Psi}] = \begin{bmatrix} 1{\cdot}0 & 1{\cdot}0 & 1{\cdot}0 \\ 1{\cdot}41 & 0{\cdot}0 & -1{\cdot}41 \\ 1{\cdot}0 & -1{\cdot}0 & 1{\cdot}0 \end{bmatrix},$$

where $[\boldsymbol{\Psi}]$ is the normalized mode shape matrix. The mass normalized mode shape matrix $[\boldsymbol{\Phi}]$ can be determined from applying the formula [31]

$$[\boldsymbol{\Phi}] = [[\mathbf{m}_r]^{1/2}]^{-1}[\boldsymbol{\Psi}],$$

where $[\mathbf{m}_r]$ is the diagonal modal mass matrix and may be calculated from

$$[\mathbf{m}_r] = [\boldsymbol{\Psi}]^{\mathrm{T}}[\mathbf{m}][\boldsymbol{\Psi}].$$

The value of the matrix $[\boldsymbol{\Phi}]$ is found to be

$$[\boldsymbol{\Phi}] = \begin{bmatrix} -0{\cdot}5 & 0{\cdot}707 & -0{\cdot}5 \\ -0{\cdot}707 & 0{\cdot}0 & 0{\cdot}707 \\ -0{\cdot}5 & -0{\cdot}707 & -0{\cdot}5 \end{bmatrix}.$$

A step input force of magnitude 0·1 N is applied at mass 1 and the displacement output response at the three masses are calculated using the mode superposition method [32]. The time and frequency responses at mass 3 are presented in Figure 2 which shows the system natural frequencies.

The matrix $[\mathbf{S}]_{gg}$ is found from these displacement data utilizing equation (2.40). Then the PCA procedure is implemented to factorize the matrix $[\mathbf{S}]_{gg}$, and obtain the matrix $[\mathbf{U}]$ as

$$[\mathbf{U}] = \begin{bmatrix} -0{\cdot}5 & 0{\cdot}712 & -0{\cdot}493 \\ -0{\cdot}707 & -0{\cdot}0008 & 0{\cdot}707 \\ -0{\cdot}5 & -0{\cdot}702 & -0{\cdot}51 \end{bmatrix}.$$

It is clear that the vectors of the matrix $[\mathbf{U}]$ are approximately similar to the vectors of the matrix $[\boldsymbol{\Phi}]$. Thus, one can use the matrix $[\mathbf{U}]$ to decouple the coupled displacement data to three single-d.o.f. systems as shown in Figure 3. From these graphs or their corresponding frequency response functions, it is possible to estimate the system natural frequencies as $f_{n1} = 12{\cdot}1094$ Hz, $f_{n2} = 22{\cdot}4609$ Hz, $f_{n3} = 29{\cdot}4922$ Hz, which are similar to the system natural frequencies. As a result, these natural frequencies and the eigenvectors of the matrix

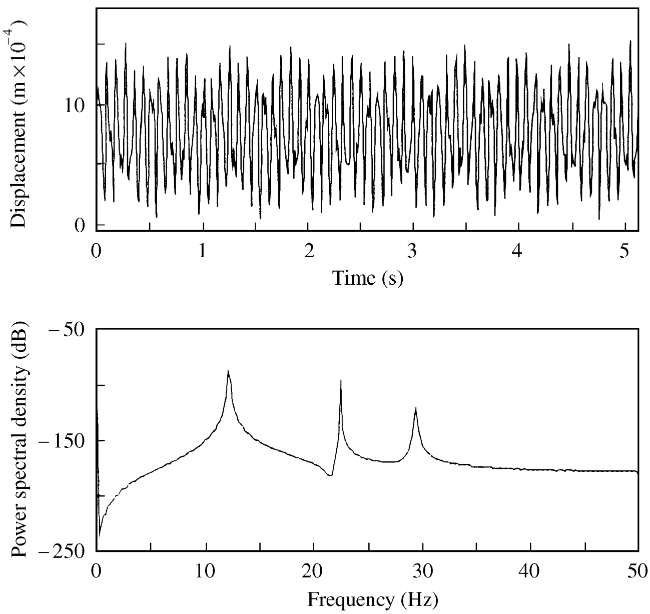

Figure 2. Time response of the three-d.o.f. structure obtained at mass 3 with the corresponding frequency response.

[**U**] can be used to calculate accurately the systems coupled displacement outputs by equation (2.46).

Furthermore, the estimated parameters are used to calculate the system response and the required optimal control signal using equations (4.2) and (4.3) via the Matlab control toolbox [33]. Here, the weighting matrices [**Q**] and [**R**] are chosen according to the discussion presented in section 3, so that the value of $[\tilde{\mathbf{Q}}]/[\mathbf{R}] \Rightarrow \infty$. The calculated control signal is introduced in the system after a delay time of 2·56 s from the starting time of simulation to suppress its vibration as shown in Figure 4. In this case, the control actuator and the detection sensor are both fixed at mass 1, i.e., the location where the input force is applied. It can be concluded here that the suggested procedure works well in controlling an unknown full order system.

Moreover, the location of the control actuator and the chosen detection sensor are going to be changed to study their effect on achieving good global minimization of the masses motions. The control actuator is placed at masses 2 and 3 while the detection sensor is chosen to be placed at mass 1. The results in time and frequency response function are presented in Figures 5 and 6 respectively. It is observed that a bad vibration cancellation appears when the control actuator is fixed at mass 2. This is due to the fact that this location is near a node for the second mode. Thus, the controller fails to suppress completely the second natural frequency as illustrated in Figure 6. However, as mass 3 is vibrating at all the systems' three natural frequencies, the vibration cancellation is quite good as shown in Figure 5. From these investigations, one can infer that the control actuator should be located at locations where the contribution of the mode shapes is maximum. The mode shapes and their contributions at each mass of the considered system that are attained for the system modes are shown in Figure 7; the mode contributions are determined by summing the absolute values of mode shapes of all the considered modes at the same mass. This rule is used with all the remaining simulation examples. Furthermore, similar results are obtained when the location of the detection sensor is changed while the control actuator is placed at the optimal location at mass 1 as shown in Figures 8 and 9. It should be noted

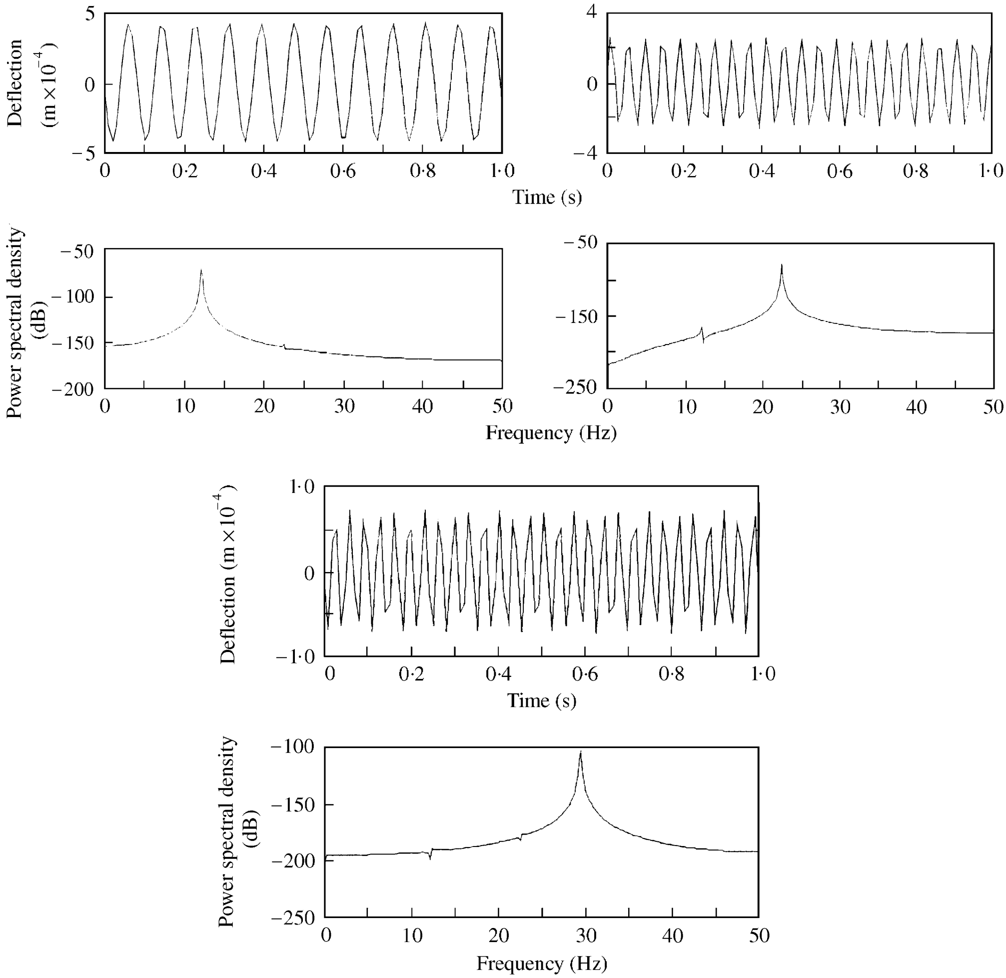

Figure 3. The principal time and frequency responses of the simulated three-d.o.f. system.

that the disturbance force is assumed to be placed at mass 1 where the maximum contribution of the mode shapes is present.

5.2. A FIVE-d.o.f. SYSTEM

The mass and stiffness of a simulated five-d.o.f. system are

$$[\mathbf{m}] = \begin{bmatrix} 1 & 0 & 0 & 0 & 0 \\ 0 & 1 & 0 & 0 & 0 \\ 0 & 0 & 1 & 0 & 0 \\ 0 & 0 & 0 & 1 & 0 \\ 0 & 0 & 0 & 0 & 1 \end{bmatrix} (\mathrm{kg}), \quad [\mathbf{k}] = \begin{bmatrix} 2 & -1 & 0 & 0 & 0 \\ -1 & 2 & -1 & 0 & 0 \\ 0 & -1 & 2 & -1 & 0 \\ 0 & 0 & -1 & 2 & -1 \\ 0 & 0 & 0 & -1 & 2 \end{bmatrix} (\mathrm{N\,m^{-1}} \times 10^4).$$

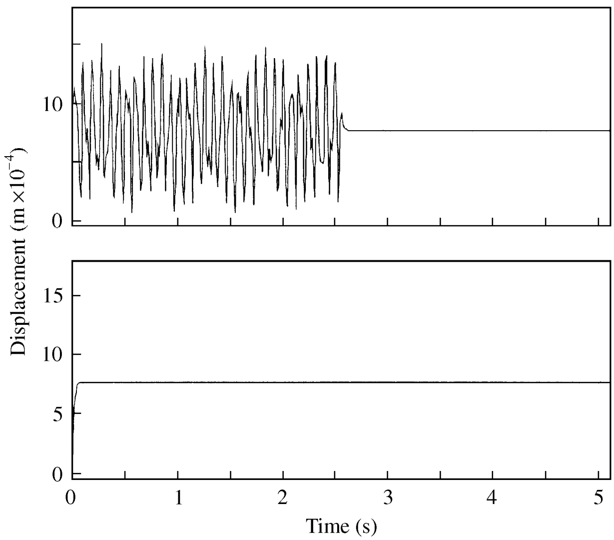

Figure 4. The controlled structure measured response at mass 3.

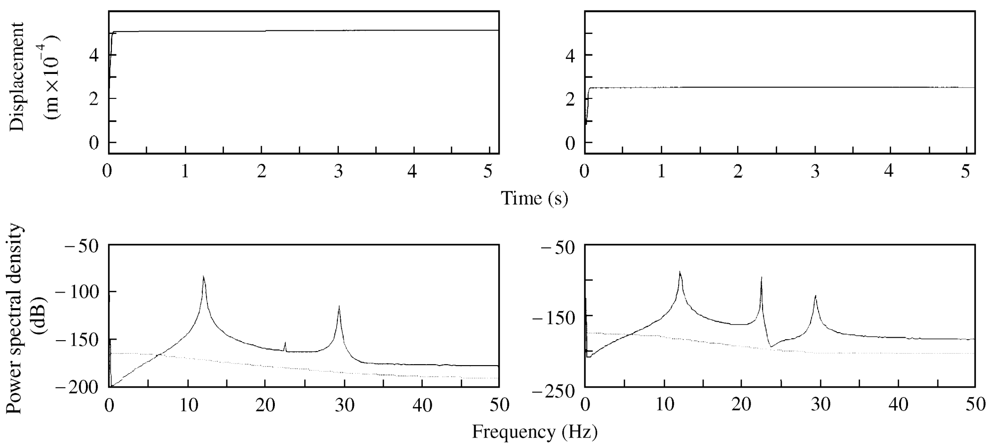

Figure 5. The structure responses when the disturbance force and detection sensor are both located at mass 1 and the controller is placed at mass 3: ——, before cancellation; - - - - - -, after cancellation. Left side shows the response of mass 1, right side refers to mass 2.

The system natural frequencies and their corresponding normalized and mass normalized mode shapes are found to be $f_{n1} = 8{\cdot}2385$ Hz, $f_{n2} = 15{\cdot}9155$ Hz, $f_{n3} = 22{\cdot}5079$ Hz, $f_{n4} = 27{\cdot}57$ Hz, $f_{n5} = 30{\cdot}74$ Hz,

$$[\boldsymbol{\Psi}] = \begin{bmatrix} 0{\cdot}5 & 1{\cdot}0 & 1{\cdot}0 & 1{\cdot}0 & 0{\cdot}5 \\ 0{\cdot}87 & 1{\cdot}0 & 0{\cdot}0 & -1{\cdot}0 & -0{\cdot}87 \\ 1{\cdot}0 & 0{\cdot}0 & -1{\cdot}0 & 0{\cdot}0 & 0{\cdot}0 \\ 0{\cdot}87 & -1{\cdot}0 & 0{\cdot}0 & 1{\cdot}0 & 0{\cdot}0 \\ 0{\cdot}5 & -1{\cdot}0 & 1{\cdot}0 & -1{\cdot}0 & 1{\cdot}0 \end{bmatrix},$$

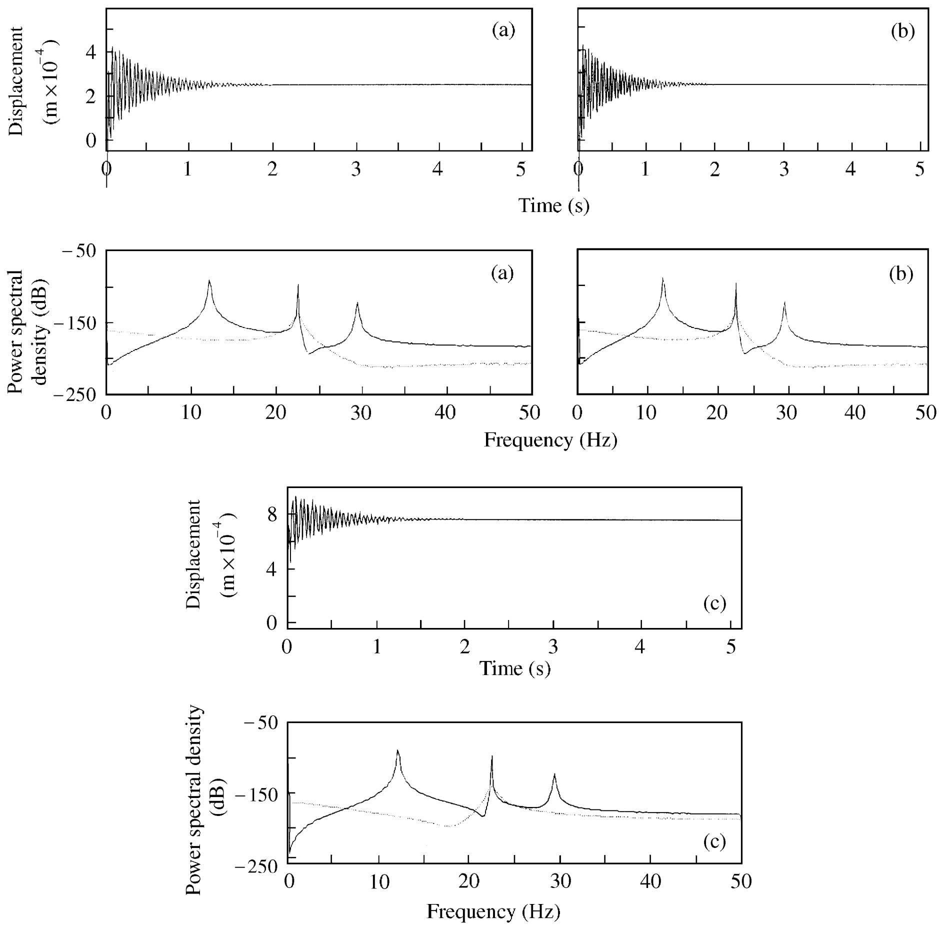

Figure 6. The structure responses when both the disturbance force and the detection sensor are located at mass 1 and the control actuator is placed at mass 2: ——, before cancellation; - - - - - -, after cancellation. (a) refers to mass 3, (b) to mass 2 and (c) to mass 1.

$$[\boldsymbol{\Phi}] = \begin{bmatrix} -0{\cdot}29 & -0{\cdot}50 & -0{\cdot}58 & -0{\cdot}58 & -0{\cdot}29 \\ -0{\cdot}50 & -0{\cdot}50 & 0{\cdot}0 & 0{\cdot}50 & 0{\cdot}43 \\ -0{\cdot}58 & -0{\cdot}0 & 0{\cdot}58 & 0{\cdot}0 & -0{\cdot}58 \\ -0{\cdot}50 & 0{\cdot}50 & 0{\cdot}0 & -0{\cdot}58 & 0{\cdot}43 \\ -0{\cdot}29 & 0{\cdot}50 & -0{\cdot}58 & 0{\cdot}58 & -0{\cdot}29 \end{bmatrix}.$$

The mode shapes and their contributions at each mass are shown in Figure 10. The graph indicates that the best locations for the control actuator and detection sensor should be at mass 1 and/or 5. A step input force of 0·1 N is applied at mass 1 and the output displacement responses are recorded at all the masses with only the first three natural frequencies included in the calculated data. The factorization of the matrix $[\mathbf{S}]_{gg}$ reveals the following

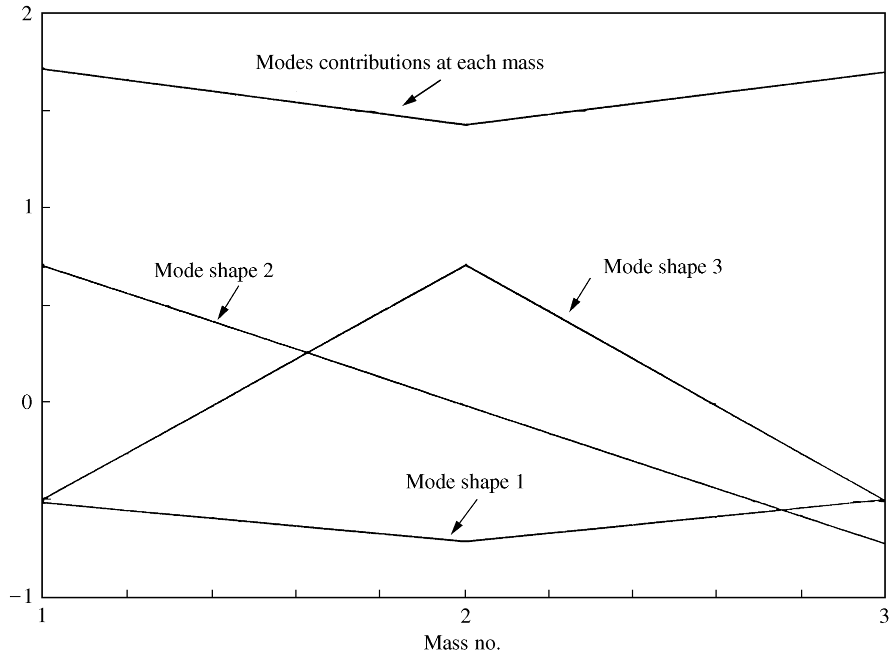

Figure 7. Modes shapes and contributions at all the masses of a three-d.o.f. system.

[**U**] matrix:

$$[\mathbf{U}] = \begin{bmatrix} -0{\cdot}288 & -0{\cdot}502 & -0{\cdot}5776 & -0{\cdot}5647 & -0{\cdot}119 \\ -0{\cdot}4991 & -0{\cdot}501 & -4{\cdot}3\times10^{-4} & 0{\cdot}706 & -3{\cdot}82\times10^{-2} \\ -0{\cdot}5772 & -1{\cdot}1\times10^{-3} & 0{\cdot}5775 & 0{\cdot}3859 & 0{\cdot}4295 \\ -0{\cdot}501 & 0{\cdot}4991 & 3{\cdot}7\times10^{-5} & -3{\cdot}8\times10^{2} & -0{\cdot}7081 \\ -0{\cdot}2898 & 0{\cdot}4995 & -0{\cdot}577 & 0{\cdot}1756 & 0{\cdot}36 \end{bmatrix}.$$

It is clear that the first three vectors of the matrix [**U**] are similar to the ones given in matrix [**Φ**]. The remaining two vectors in the [**U**] matrix represent the contribution of the last two natural frequencies that are not included in the data. The natural frequencies of the decoupled system as estimated from these data are found to be $f_{n1} = 8{\cdot}212$ Hz, $f_{n2} = 15{\cdot}925$ Hz, $f_{n3} = 22{\cdot}495$ Hz. These values are similar to the first three natural frequencies of the system. The estimated three natural frequencies and their corresponding orthonormal mode shapes [**U**] are used to construct the coupled data. Figure 11 shows the coupled data in time and frequency domains as measured at mass 4.

Consequently, the control signal is calculated and passed to the system via the control actuator which is placed at mass 1 (collocated with the detection sensor) after 2·56 s from the starting time of simulation. A good cancellation of the system vibration is accomplished as illustrated in Figure 12. It is worth mentioning that the simulation was carried out for 5·12 s.

Then, the controller is invoked from the starting time of simulation; the overall results are shown in Figure 13 as measured at all the masses of the structure. These results demonstrate and confirm the capability of the suggested procedure and control strategy used to

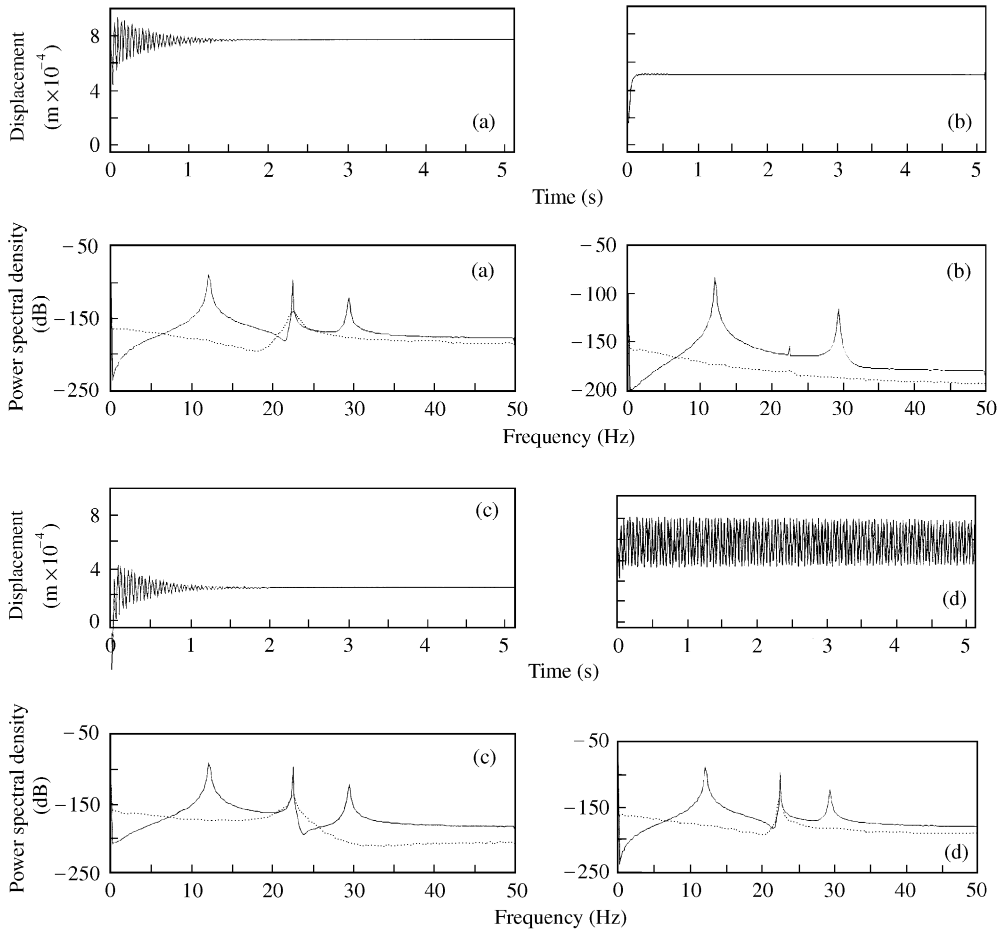

Figure 8. The structure responses when the disturbance force and the controller are both located at mass 1 and the detection sensor is placed at mass 2: ——, before cancellation; - - - - - , after cancellation. (a) refers to mass 1 with mode 2 relatively unobservable; (b) to mass 2; (c) to mass 3 and (d) to mass 1 with mode 2 completely unobservable.

efficiently control vibration in the structure where global minimization at the masses is achieved.

The effectiveness of the controller in vibration cancellation for non-collocated control actuator and detection sensor is now examined. The control actuator and the detection sensor are attached at masses 1 and 5 respectively. The selected locations are chosen to satisfy mode contribution conditions presented in Figure 10. Figure 14 shows the structure responses at masses 1, 3 and 5 where considerable cancellation is achieved, which is highly similar to that as shown in Figure 13. This is expected since the mode shape in the selected locations of control actuator and detection sensor for all the considered modes are similar.

5.3. SIMPLY SUPPORTED BEAM

An aluminium beam of 0·8 m length and cross-sectional area of $2{\cdot}1894 \times 10^{-5}$ m is used as a practical example. The beam is modelled as a 28-d.o.f. system where the elements of the

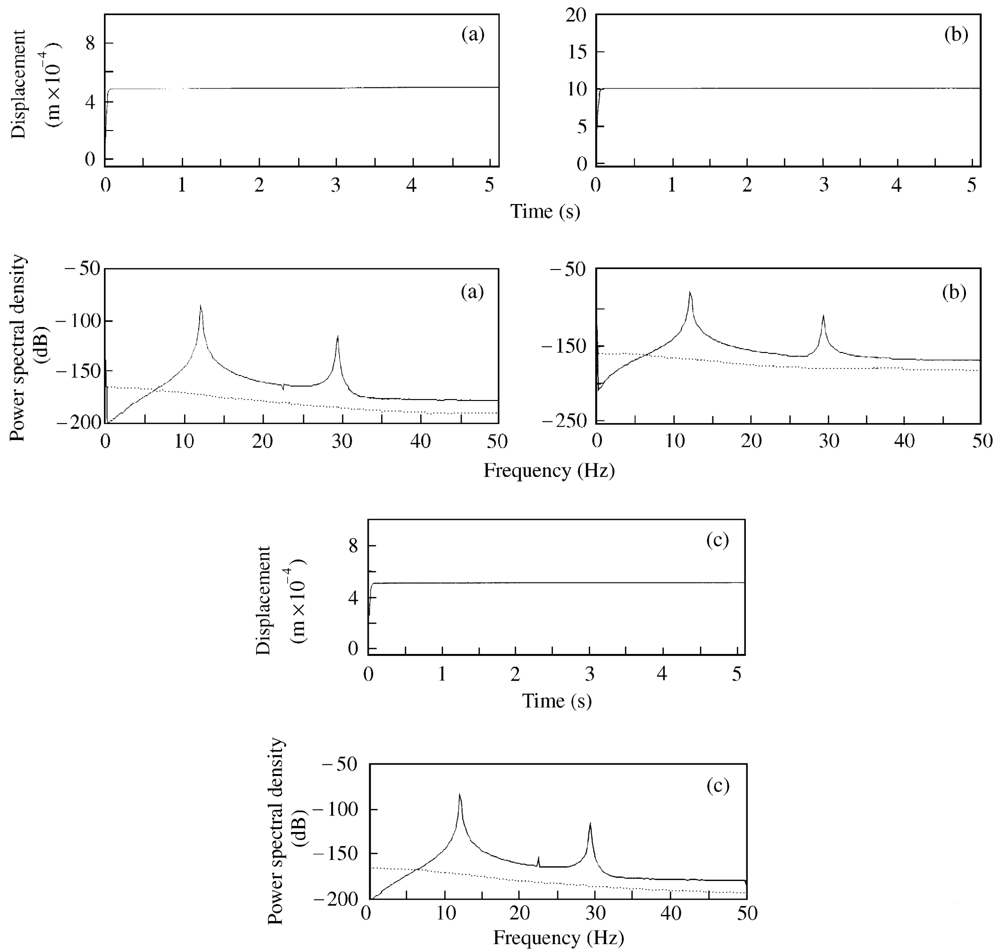

Figure 9. The structure responses when the disturbance force and the controller are both located at mass 1 and the detection sensor is placed at mass 3: ——, before cancellation; - - - - - -, after cancellation. (a) refers to mass 1; (b) to mass 2 and (c) to mass 3.

flexibility matrix $[\boldsymbol{\delta}]$ can be found using the formula form reference [24]

$$\delta_c = ((l-a)/6EIl)\,(l^2x - x^3 - (l-a)^2x) \quad \text{for } x \leqslant a, \tag{5.1}$$

where a is the distance of the unit applied force from the left support, EI is the modulus of rigidity of the beam, x is the distance with respect to the left support of the beam of length l.

Similarly, in digitized form, it can be written as

$$\delta_{c\eta} = ((N_s + i + 1)/6EI(N_s + 1))\, l^3 \{[(N_s + 1)^2 i - j^3] - [(N_s - i + 1)^2 \times j]\},$$

$$i = N_s, N_s - 1, \ldots, 1, \quad j = i, i-1, \ldots, 1, \tag{5.2}$$

where N_s is the number of segments and $\delta_{c\eta} = \delta_{c\eta}$.

Since the stiffness matrix $[\mathbf{K}]$ is the inverse of $[\delta]$, one can adopt a Gaussian elimination routine to obtain $[\mathbf{K}]$ from $[\boldsymbol{\delta}]$, therefore,

$$[\mathbf{K}] = [\boldsymbol{\delta}]^{-1}. \tag{5.3}$$

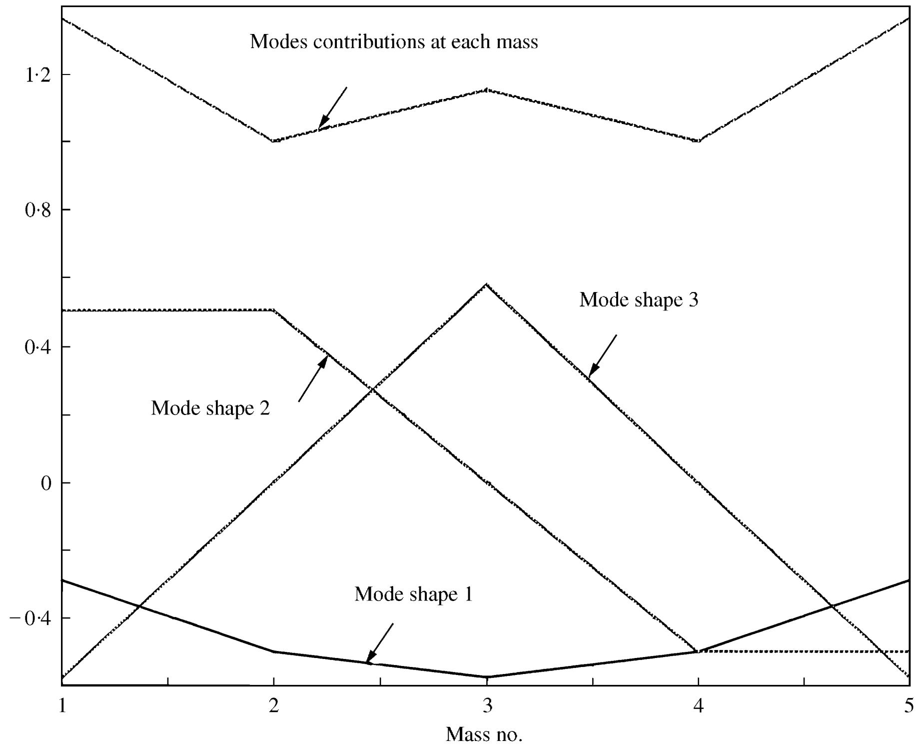

Figure 10. Modes shapes and contributions at all the masses of a five-d.o.f. system.

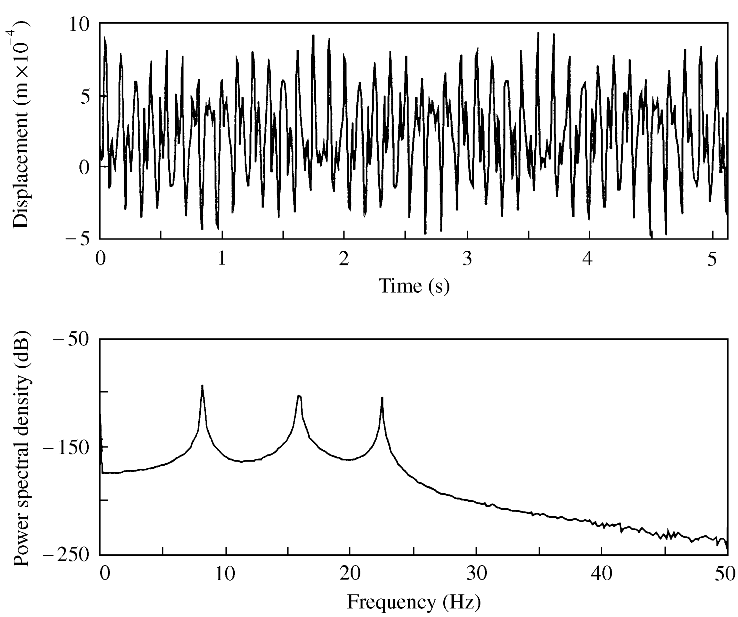

Figure 11. The response of the five-d.o.f. structure in time and frequency domains as measured at mass 4.

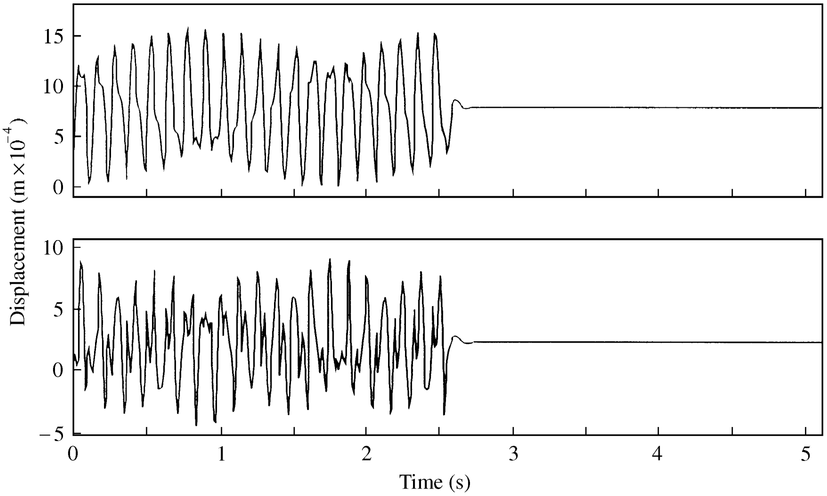

Figure 12. The controlled structure responses as measured at masses 4 and 1 respectively.

In addition, the diagonal mass matrix [**M**] can be constructed by assuming that the mass of each segment is concentrated at its mid-span. Thus, the mass elements of the simply supported beam may be obtained using

$$m(i, i) = \rho \Delta l, \quad i = 1, 2, 3, \ldots, N_s, \tag{5.4}$$

where ρ is the mass per unit length. The first three natural frequencies of the system are found using the calculated mass and stiffness matrices, being: $f_{n1} = 8{\cdot}2385$ Hz, $f_{n2} = 15{\cdot}9155$ Hz, $f_{n3} = 22{\cdot}5079$ Hz and their corresponding normalized mode shapes are presented in Figure 15. A disturbance force of 0·1 N is assumed to be applied at 0·22 m from the left support of the beam to excite the system with only the first three modes included in the calculated data. The estimated natural frequencies are found in a similar way as for the above examples where they are found to be $f_{n1} = 8{\cdot}253$ Hz, $f_{n2} = 15{\cdot}897$ Hz, $f_{n3} = 22{\cdot}511$ Hz. The control strategy discussed in section 4 is again implemented for vibration cancellation of such structures. The positions of detection sensor and control actuator are chosen according to the results presented in Figure 15. The time and frequency responses calculated at location 0·35 m are as shown in Figure 16.

To assess the behavior of the controller upon vibration cancellation over the entire beam length, the controller and the detection sensor are both located at location 0·35 m for the collocated case. Figure 17 shows that a significant reduction in the vibration level has been achieved throughout the length of the beam where the controller is turned on after 2·56 s from the starting time of simulation. In addition, this result demonstrates that the controller and the modal model work well for such a purpose. Figure 18 and 19 show the time and frequency domains of the behavior of the controlled beam along its length for collocated and non-collocated cases respectively.

The average power spectral density throughout the length of the beam before and after cancellation for collocated case is given in Figure 20. The average attenuation over all the considered modes is found to be 43·93 dB. It is clear that a similar performance can be attained for the uncollected case where the attenuation is found to be 43·5 dB. Consequently, it is worth mentioning that the kinks in the graph in Figure 20 indicate the modal nodes.

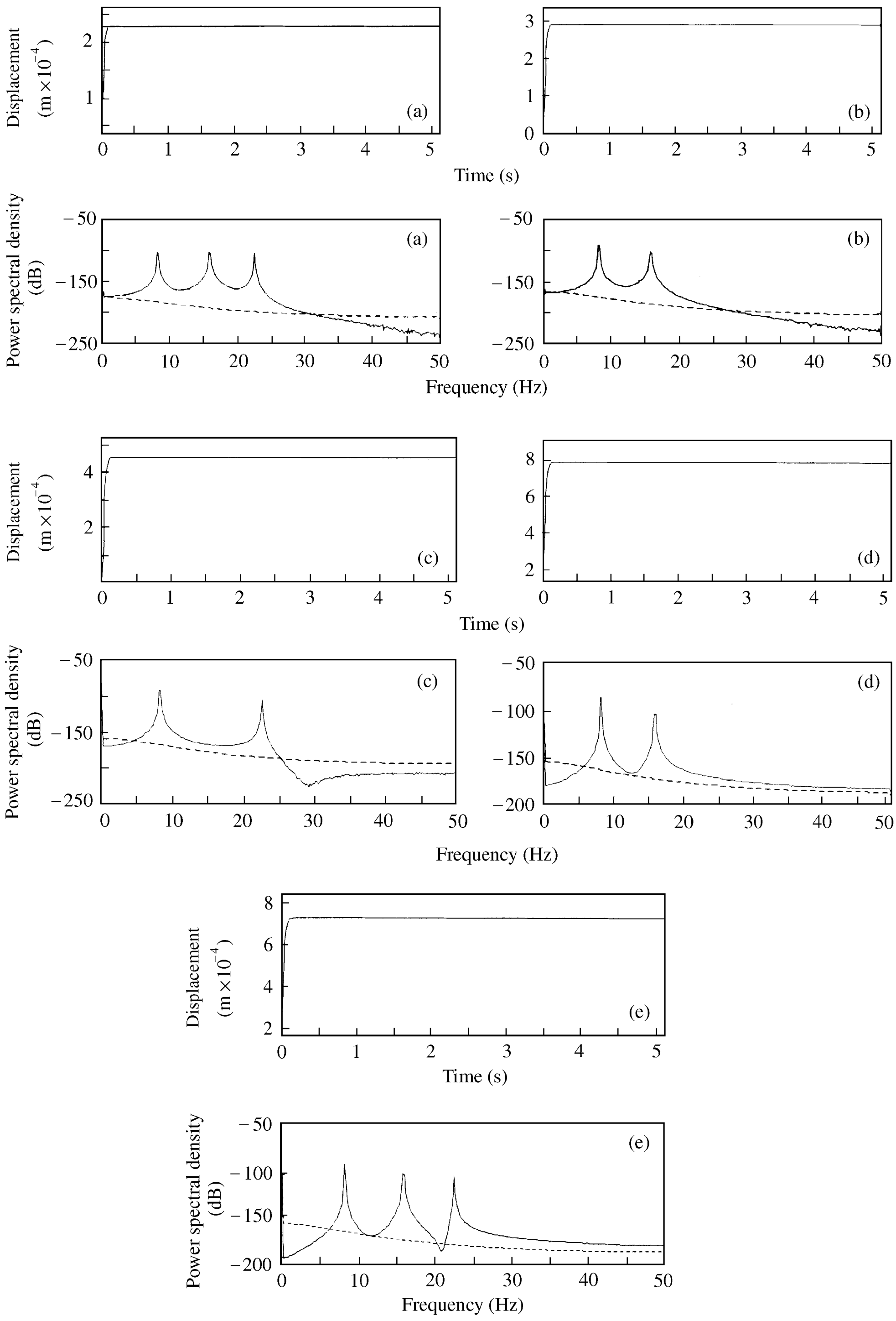

Figure 13. The controlled structure responses within time and frequency domains measured at all the masses along the structure: ——, before cancellation; - - - - - -, after cancellation. (a) refers to mass 1; (b) to mass 2; (c) to mass 3; (d) to mass 4 and (e) to mass 5.

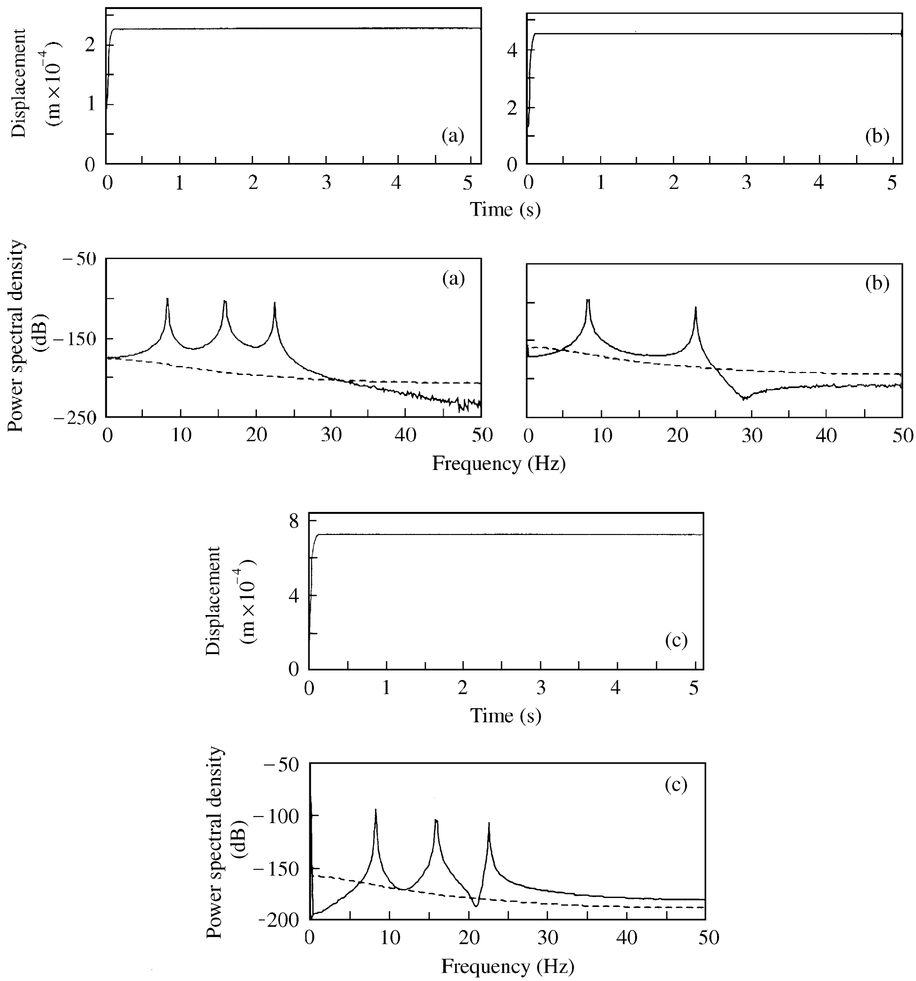

Figure 14. The controlled structure responses within time and frequency domains measured at some selected masses for the non-collocated control actuator and detection sensor: ——, before cancellation; ------, after cancellation. (a) refers to mass 1; (b) to mass 3 and (c) to mass 5.

6. CONCLUSIONS

In this paper, principal component analysis (PCA) was introduced as a technique to estimate the natural frequencies and the mode shapes for the structures under consideration. PCA was found to have two main advantages; first, it has the ability to produce effectively single-d.o.f. data with well-separated resonances and secondly, it minimizes the effect of the residual modes. The estimated parameters were utilized in designing the modal model and controlling the vibration of such structures. The control law was designed using state-space representation and tested on three- and five-d.o.f structures as well as on a simply supported beam structure. The results demonstrate the successful implementation of an optimal control strategy for cancelling the vibration. The control technique was successfully carried out for collocated and non-collocated control actuator/detection sensor locations. Further studies for the determination of the control actuator and the detection sensor suitable locations has been investigated. A simple way for

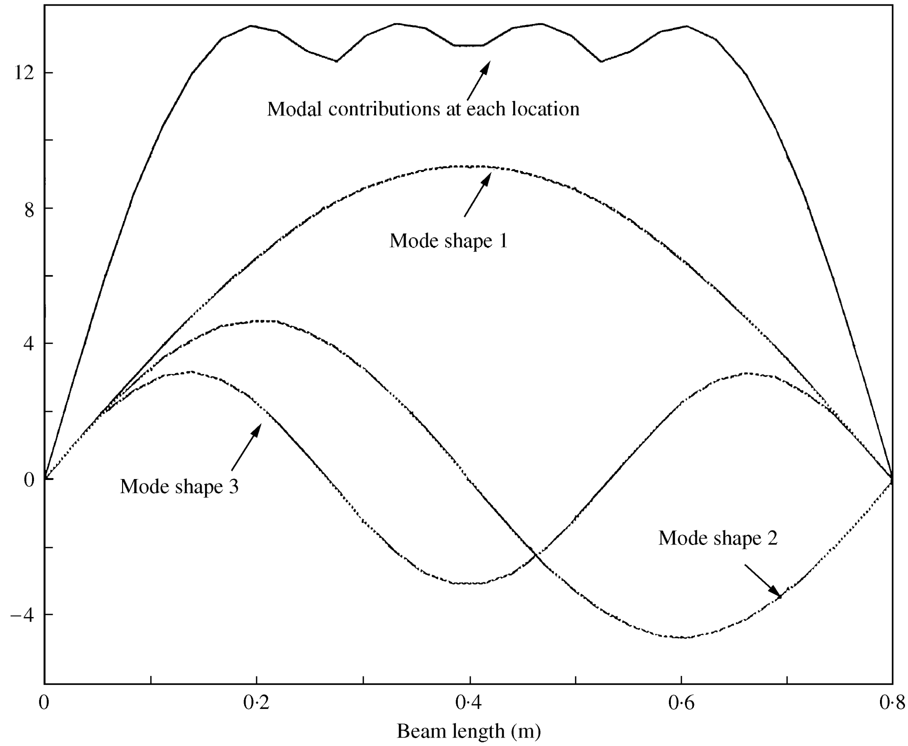

Figure 15. Modes shapes and contribution throughout the length of a simply supported beam structure.

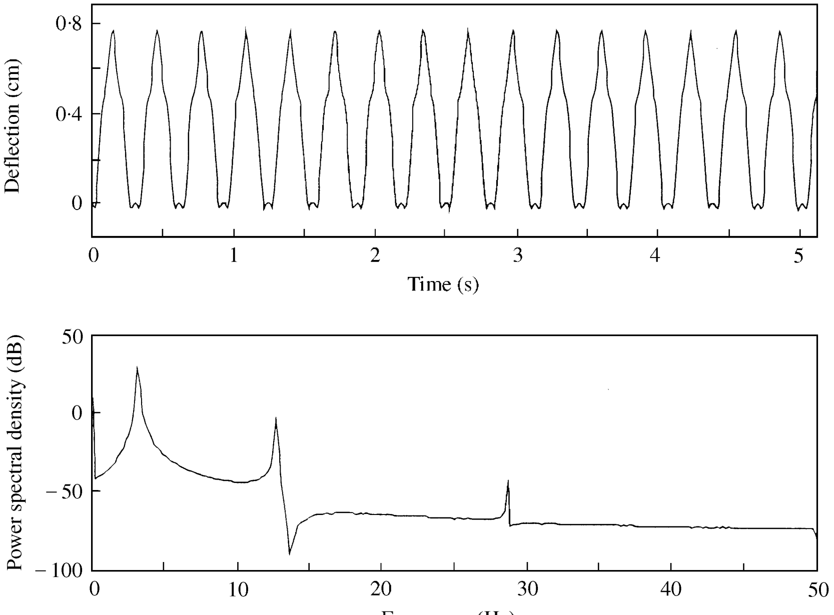

Figure 16. Time and power spectral density responses of uncontrolled simply supported beam measured at location 0·35 m.

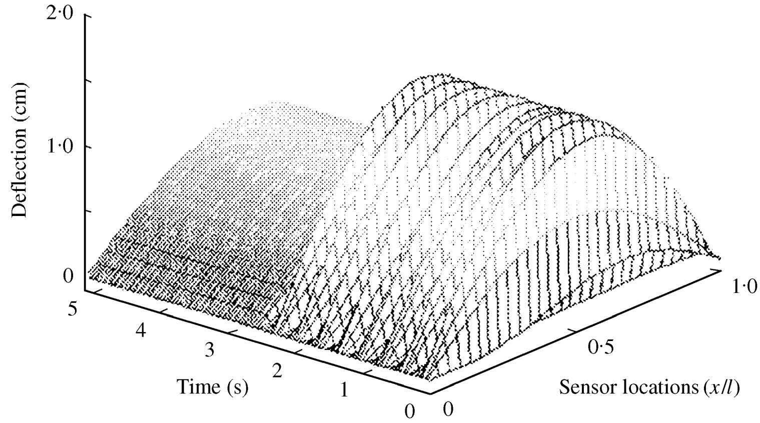

Figure 17. Beam response before and after cancellation when the controller is turned on after 2·56 s.

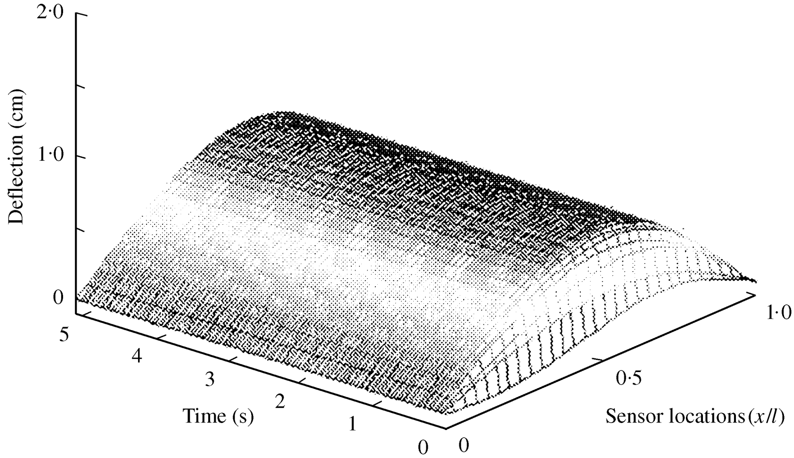

Figure 18. Beam response along its length after cancellation for collocated case.

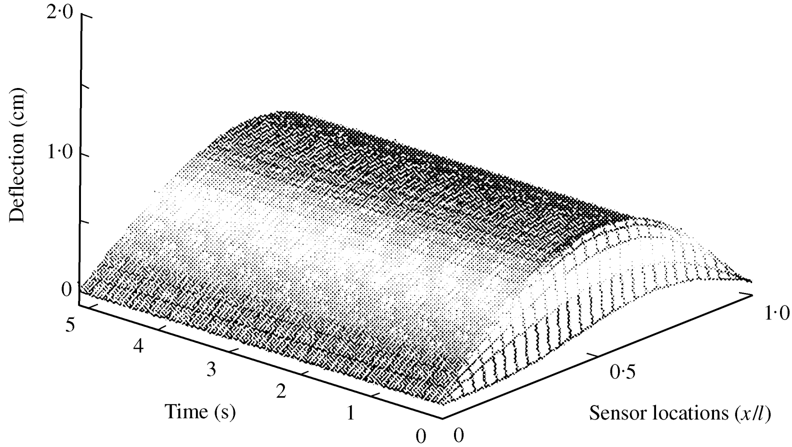

Figure 19. Beam response along its length after cancellation for non-collocated case.

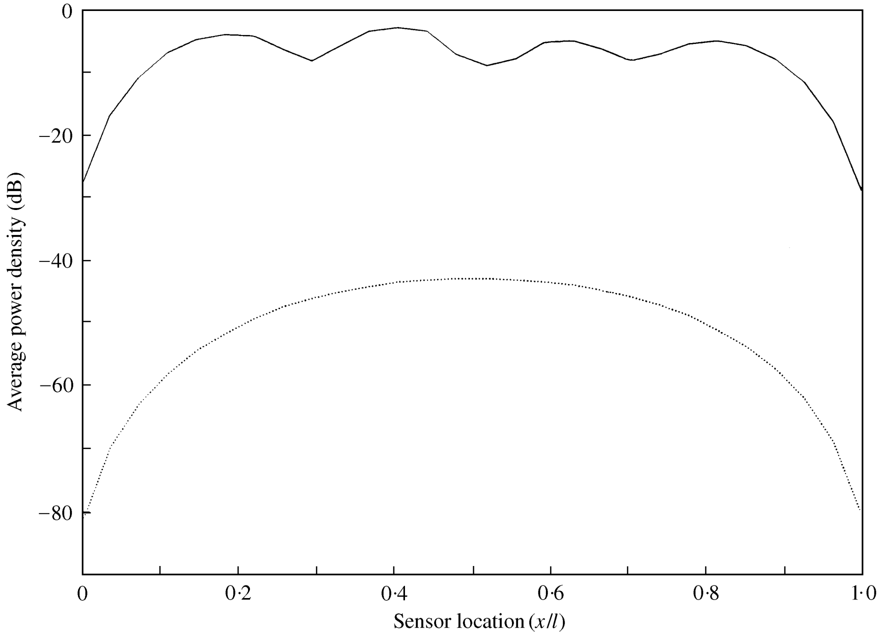

Figure 20. Average power spectral density for the collocated case: ——, before cancellation; ------, after cancellation.

specifying such suitable positions was based on calculating the mode shapes continuations at the lumped masses. It is worth mentioning here that, a comparison was carried out between this proposed method and other techniques, which did not require prior knowledge of the model such as fuzzy logic and genetic algorithm and will be published in the future. This work shows that the presented procedure is successful in vibration suppression of flexible structures when compared with the other methods. In view of the simulation results, it can be concluded with some confidence that the PCA procedure with active control strategies offers a viable solution for vibration problems.

REFERENCES

1. A. S. Al-Dmour 1996 *Ph.D. Thesis, University of Bradford*. Active controllers for vibration suppression in flexible beam structures.
2. J. G. Webb 1993 *Proceedings of Damping* 93', Vol. 3, IBCI-18. Comparing passive damping and active control on flexible structure with either closely spaced or coincident modes.
3. L. Y. Pao and G. F. Franklin 1990 *Proceedings of the* 29*th Conference on Decision and Control*, 2580–2581. Time-optimal control of flexible structures.
4. D. Dosch, D. Leo and D. Inman 1995 *Journal of Guidance, Control, and Dynamics* **18**, 340–346. Modeling and control for vibration suppression of a flexible active structure.
5. L. A. Sievers and A. H. Von Flotow 1988 *Proceedings of the* 27*th Conference on Decision and Control*, 1032–1037. Linear control design for active vibration isolation of narrow band disturbances.
6. S. D. Snyder and N. Tanaka 1995 *IEEE Transactions on Neural Networks* **6**, 819–829. Active control of vibration using a neural networks.
7. Q. Zhang, S. Shelley and R. Allemang 1991 *Journal of Dynamic systems, Measurement and Control* **113**, 259–265. Active damping of flexible structures based on SISO and SIMO non-collocated sensor–actuator velocity feedback.
8. K. S. Mohammad and A. S. Al-Dmour 2001 Active vibration suppression of lumped modeled flexible structures (in press).

9. P. K. KOURMOULIS 1990 *Ph.D. Thesis, University of Sheffield*. Parallel processing in the simulation and control of flexible beam structure systems.
10. F. N. ALGHANNAM 1995 *Ph.D. Thesis, University of Bradford*. Parallel computing for the simulation of vibration beam structures.
11. B. PORTER and R. CROSSLEY 1972 *Modal Control Theory and Applications*. London: Taylor & Francis.
12. M. J. BALAS 1978 *IEEE Transactions on Automatic Control* **33**, 673–5679. Feedback control of flexible systems.
13. M. O. TOKHI and M. A. HOSSAIN 1994 *Journal of Systems and Control Engineering* **208**, 236–277. Self-tuning active vibration control in flexible beam structures.
14. G. S. VIRK and A. S. AL-DMOUR 1999 *Microprocessors and Microsystems* **23**, 365–384. Real-time vibration suppression in a flexible cantilever rig.
15. A. S. AL-DMOUR 1999 *Mu'tah Journal for Research and Studies "Natural and Applied Science Series"* **14**, 37–58. Active vibration suppression in a flexible cantilever beam using fuzzy logic controllers.
16. A. S. AL-DMOUR 2000 *Natural and Engineering Sciences, The University of Jordan* **27**, 110–124. Improved fuzzy logic controller using genetic algorithm and its application to vibration suppression of flexible structures.
17. A. BAZ, S. POH and J. FEDOR 1989 *Journal of Mechanical Engineering Science* **203**, 103–112. Independent modal space control with positive position feedback.
18. A. BAZ, S. POH and P. STUDER 1992 *Transaction of ASME, Journal of Dynamic Systems, Measurement and Control* **114**, 97–103. Modified independent modal space control for active control method of flexible systems.
19. L. A. GOULD and M. A. MURRAY-LASSON 1964 *IEEE Transactions on Automatic Control* 729–737. On the modal control of the distributed systems with distributed feedback.
20. D. J. INMAN 1989 *Vibration with Control Measurements and Stability*. Englewood Cliffs, NJ: Prentice-Hall.
21. H. G. GOYDER 1984 *Short Course Notes, University of Manchester*. Vibration analysis and identification of non-linear structures.
22. S. R. IBRAHIM and E. C. MIKULCIK 1977 *Shock and Vibration Bulletin* **47(4)**, 183–198. A method for the direct identification of vibration parameters for the free response.
23. J. LEURIDAN 1984 *Ph.D. Dissertation, University of Cincinnati*. Some direct parameter model identification methods applicable for multiple input modal analysis.
24. K. S. MOHAMMAD 1990 *Ph.D. Thesis, Heriot-Watt University*. Identification of the characteristics of the non-linear structures.
25. K. PEARSON 1901 *Philosophical Magazine* **2**, 559–572. On lines and planes of closet fit systems of points in space.
26. H. HOTELLING 1933 *Journal of Educational Psychology* **24**, 417–441, 498–520. Analysis of complex statistical variables into principal components.
27. G. B. THOMAS 1968 *Calculus of Analytical Geometry*. Reading, MA: Addison-Wesley.
28. G. E. FORSYTHE, M. A. MALCOLM and C. B. MOLER 1978 *Computer Methods for Mathematical Computations*. Englewood Cliffs, NJ: Prentice-Hall.
29. J. S. TYLER 1964 *IEEE Transactions on Automatic Control* 485–498. The characteristics of the model-following systems as synthesized by optimal control.
30. L. MERIOVITCH, H. BARUH and H. OZ 1983 *Journal of Guidance* **6**, 303–310. A comparison of control techniques for large flexible systems.
31. F. S. TSE and I. E. MORSE 1978 *Mechanical Vibration*. Needham Heights, MA: Allyn & Bacon.
32. B. R. CRAIG 1981 *Structural Dynamics: An Introduction to Computer Methods*. New York: John Wiley and Sons.
33. A. GRACE, A. J. LAUB, J. N. LITTLE and C. M. THOMPSON 1992 *The Math Works Inc*. Control system toolbox for use with Matlab.